10th World Congress on Structural and Multidisciplinary Optimization
May 19 -24, 2013, Orlando, Florida, USA

Minimizing Machinery Vibration Transmission in a Lightweight Building using Topology Optimization

Niels Olhoff, Bin Niu

Department of Mechanical and Manufacturing Engineering, Aalborg University, DK-9220 Aalborg, Denmark

1. Abstract
This paper deals with the problem of minimizing the vibration transmission in a lightweight building from rotating machinery, by topological design of a flexible base plate for the machinery. A modular lightweight building is modeled and used for the analysis of the vibration transmission. The design objective is chosen as minimization of the product of the frequency response in the building transmitted from the machinery via walls and floors, and the volume of material used in the design of the base plate. Different excitation frequencies are considered. The design and performance of the optimized machinery base plates are illustrated and discussed via numerical examples.
2. Keywords: Machinery, Topology optimization, Lightweight building, Vibration, Base plate.

3. Introduction
Due to the existence of dynamic forces of e.g. mechanical, fluid dynamic or electro-magnetic origin, rotating machinery may be considered a source that excites forced vibration of the foundation, and thereby the floors and walls, etc., of the building. The transmission of such vibrations through the building may result in undesirable sound emission and unsatisfactory comfort conditions for the people in dwellings and offices of the building. To remedy this, the objective of this work is to develop and implement a method of topology optimization for the design of a machinery foundation.
Hence, this paper studies the coupled system of the machinery installation and the building. We propose that the foundation of the machinery should be a flexible, single-material base plate that is topology optimized within a quadratic, admissible design domain which is supported by the floor of a storey or the roof of the building, and minimizes the vibration transmission in the building. The reader is referred to the machinery installation indicated on top of Room 2-3 in Figure 1 with a close-up in the right-hand side showing the machine and the quadratic, admissible design domain for its base plate.
The machine is considered to be relatively stiff (approximately considered as a rigid body), which is rigidly connected to the base plate via four bolts, and the base plate is assumed to be connected to the elastic roof (or floor) of the building by moment-free hinges at the four corners of the admissible design domain. For the convenience and consistence of implementation with the other parts, the machine is modeled as a three-dimensional elastic body with a higher Young's modulus than that of the base plate.
The design objective is chosen as minimization of the product of the frequency response in the building transmitted from the machinery via walls and floors, and the volume of material used in the design of the base plate. The product objective in the topology optimization of vibrating structures is studied in Ref. [1], which is inspired and extended from the work on "extended optimality" in Refs. [2-4] where Rozvany et al. studied the minimization of the product of the static compliance and the volume of material used.

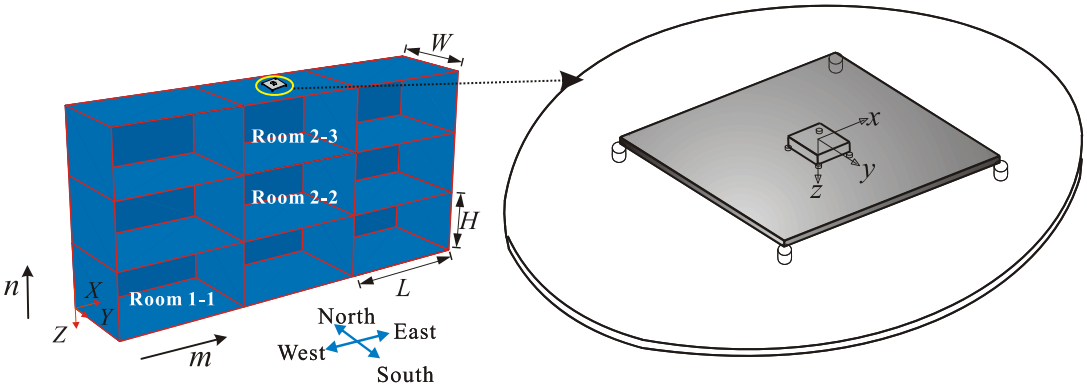

Figure 1 Schematic of building and the machinery with the quadratic admissible design domain for the base plate

In the current product formulation of simultaneously minimizing the vibration transmission in the building and the amount of material for the base plate, we found it to be expedient to specify a maximum constraint for the static displacement of the machine, since the optimization of the base plate otherwise attempts to achieve minimum frequency response (zero) of the building by separating the building from the vibration source. This trivial solution is, of course, not useful.

In this paper, the vibration transmission in the building is calculated for a modular lightweight building which is entirely constructed by translation and combination of three basic modular elements, i.e., one floor panel and two different wall panels. These panels are all considered as beam-stiffened double-leaf panels. Furthermore, an artificial skeleton is introduced to facilitate the modelling of different connections between modules in the building. More details on the implementation of the parametric modelling of a modular building are available in our companion papers [5, 6].

The organization of the rest of the paper is as follows. The optimization formulation is described in Section 4, followed by material interpolation in Section 5. Section 6 presents the sensitivity analysis of the objective and constraint functions. Numerical examples are outlined in Section 7 for different excitation frequencies and values of the maximum static displacement constraint for the machine. Finally, a section with discussions and conclusions closes the paper.

4. Optimization formulation

Since the vibration of the building is almost exclusively determined by the building alone, the topological design of the base plate has little influence on the vibration modes of the building. This means that the vibration mode of a particular receiving room cannot be influenced significantly by topological design of the base plate. However, different designs of the base plate will result in different transmitted forces on the installation floor. Therefore, the problem of minimizing the vibration transmission in the building can be considered as minimizing the magnitudes of the transmitted forces on the installation floor while prescribing different frequency-dependent boundary conditions at the four corner supports at the quadratic design domain of the base plate. The frequency-dependent boundary conditions can be determined from the forced vibration analysis of the building by applying separately a unit excitation force of the given excitation frequency at each prescribed installation point. Since the properties of the building are given, the magnitude of the transmitted forces on the installation floor can be equivalently considered by the magnitudes of the displacements of the installation points on the floor. The optimization problem for minimizing the product of the vibration transmission and the volume of material used can be reformulated as

$$
\begin{aligned}
&\underset{\rho_j}{\text{minimize}} && U^2 \bullet \frac{V}{V_0} && \text{(a)} \\
&\text{subject to} && \mathbf{K}_\mathrm{p}\mathbf{u}_\mathrm{p} + \mathbf{C}_\mathrm{p}\dot{\mathbf{u}}_\mathrm{p} + \mathbf{M}_\mathrm{p}\ddot{\mathbf{u}}_\mathrm{p} = \mathbf{f}_0 - \mathbf{f}_\mathrm{t}, && \text{(b)} \\
& && \mathbf{K}_\mathrm{b}^{\mathrm{eq}}\mathbf{u}_\mathrm{p}^\mathrm{c} = \mathbf{f}_\mathrm{t}, && \text{(c)} \\
& && g\left(\mathbf{u}_\mathrm{m}\left(\omega = 0\right)\right) \le \bar{g}, && \text{(d)} \\
& && \underline{\rho} \le \rho_j \le 1,\ j = 1, \ldots, N_\mathrm{d}. && \text{(e)}
\end{aligned}
\qquad (1)
$$

The objective function in Eq. (1a) is defined as the product of the squared displacement response U^2 at the installation points and the volume ratio $\frac{V}{V_0}$ between the volume of material $V = \sum_{j=1}^{N_\mathrm{d}} \rho_j v_j$ of the base plate, where v_j is the volume of the *j*-th element of the base plate design, and the volume of material V_0 of the admissible design domain. The design variables ρ_j, $j = 1, \ldots, N_\mathrm{d}$, represent the volumetric material densities of the finite elements, where N_d is the number of finite elements of the admissible design domain. The squared displacement response U^2 in the objective is evaluated as

$$
U^2 = \frac{1}{N_\mathrm{c}} \left|\mathbf{u}_\mathrm{p}^\mathrm{c}\right|^\mathrm{T} \left|\mathbf{u}_\mathrm{p}^\mathrm{c}\right| = \frac{1}{N_\mathrm{c}} \left(\mathbf{u}_\mathrm{p}^\mathrm{c}\right)^\mathrm{T} \bar{\mathbf{u}}_\mathrm{p}^\mathrm{c}, \qquad (2)
$$

where the vector $\mathbf{u}_\mathrm{p}^\mathrm{c}$ denotes the translational displacements of the four installation points, cf. Figure 2, and N_c is the number of the translational degrees of freedom at the installation points. The overbar denotes complex conjugate of a vector or matrix, and the superscript T represents the transpose of a matrix or vector. $\mathbf{u}_\mathrm{p}^\mathrm{c}$ is extracted from the displacement vector $\mathbf{u}_\mathrm{p}$ by introducing a location matrix $\mathbf{L}$, which is a zero matrix with unit values at

the diagonal elements corresponding to the translational degrees of freedom of the nodes of the installation points.

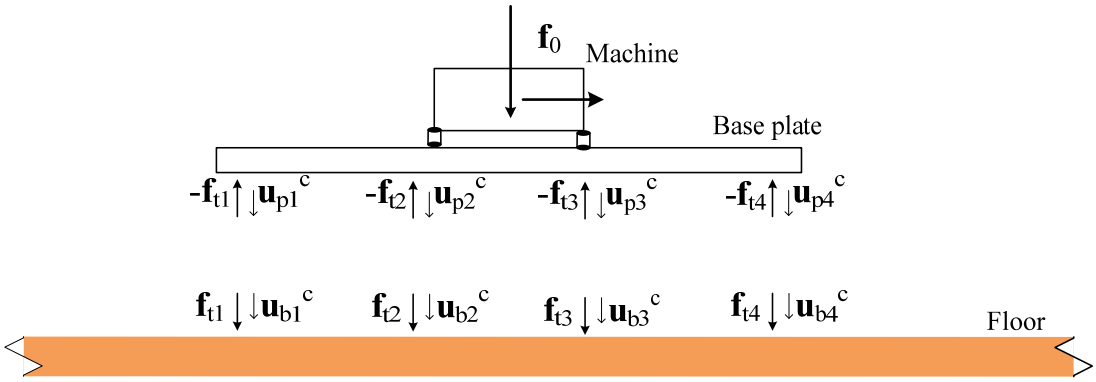

Figure 2 Schematic of machinery installation in a lightweight building

The symbols $\mathbf{K}_p$, $\mathbf{M}_p$, and $\mathbf{C}_p$ are the stiffness, the mass, and the damping matrices of the base plate with the machine, $\mathbf{u}_p$ is the displacement vector of the base plate with the machine, and $\mathbf{K}_b^{eq}$ is the frequency-dependent complex equivalent dynamic stiffness matrix of the building at the installation points. For different excitation frequencies and different installation positions in the building, different vibration modes of the building may be excited so that the response at the installation points on the building floor will be different. Therefore, $\mathbf{K}_b^{eq}$ should be computed via the forced vibration analysis of the building at each given frequency. The symbol $\mathbf{f}_0$ is the excitation force applied at the centre of gravity of the machine, and $\mathbf{f}_t$ denotes the transmitted force at the installation points on the floor where the machine is installed via the base plate. For the four installation points, the transmitted force $\mathbf{f}_t$ on the floor and the corresponding displacement vector $\mathbf{u}_b^c$ are written as

$$\mathbf{f}_t = \left\{\mathbf{f}_{t1} \quad \mathbf{f}_{t2} \quad \mathbf{f}_{t3} \quad \mathbf{f}_{t4}\right\}^T,\ \mathbf{u}_b^c = \left\{\mathbf{u}_{b1}^c \quad \mathbf{u}_{b2}^c \quad \mathbf{u}_{b3}^c \quad \mathbf{u}_{b4}^c\right\}^T. \tag{3}$$

The forces and displacements at the interface of the contiguous base plate and the floor are shown in Figure 2, where the arrows define the positive directions of the forces and the displacements. The coupling between the base plate with the machinery and the building is realized by the compatibility of the displacements, $\mathbf{u}_p^c = \mathbf{u}_b^c$.

If a fixed moment-free hinge connection is assumed at the mounting junction on the floor, only force transmission takes place , and the force vector $\mathbf{f}_{t1}$, see Figure 2, only has translational components in the *x*-, *y*-, and *z*-directions,

$$\mathbf{f}_{t1} = \left\{ f_{t1}^x, f_{t1}^y, f_{t1}^z \right\}^T. \tag{4}$$

Furthermore, if the in-plane motion of the base plate is ignored, only the vertical force in the *z*-direction should be considered. For this case, $\mathbf{K}_b^{eq}$ is reduced to a 4×4 complex matrix.

Eq. (1d) specifies a constraint on the static (ω=0) displacement of the machine which prevents a trivial solution with an unreasonably large value of this displacement. The function $g\left(\mathbf{u}_m\left(\omega=0\right)\right)$ is computed by Eq.(5) as the root-mean-square (RMS) value of the displacements of the machine, and $\bar{g}$ is the upper allowable limit for this RMS value. We have

$$g\left(\mathbf{u}_m\left(\omega=0\right)\right) = \sqrt{\frac{1}{N_m}\mathbf{u}_m^T\mathbf{u}_m}, \tag{5}$$

where $\mathbf{u}_m$ denotes the displacement vector of all degrees of freedom of the machine, and N_m is the number of the degrees of freedom of the displacements of the machine. The location matrix $\mathbf{R}$ is defined for extracting the displacement vector $\mathbf{u}_m$ of the machine from the displacement vector $\mathbf{u}_p$, i.e. $\mathbf{u}_m = \mathbf{R}\mathbf{u}_p$, cf. Sub-section 6.2.

Eq. (1e) specifies the lower and upper limits $\underline{\rho}$ and 1.0 for the design variable ρ. For this topology optimization problem with a single material, a small positive value like 0.001 is prescribed for $\underline{\rho}$ in order to avoid numerical singularity.

We assume time harmonic motion, and omit the time dependent term $\exp\left(\mathrm{i}\omega t\right)$ in the remainder. The symbol ω

denotes the excitation frequency, and i represents the imaginary unit, $\mathrm{i}=\sqrt{-1}$. Damping is important for the vibration analysis and design of lightweight buildings, but we disregard damping in this paper and assume $\mathbf{C}_\mathrm{p}=\mathbf{0}$. The optimization formulation in Eq. (1) can be rewritten as

$$\begin{aligned}
&\underset{\rho_j}{\text{minimize}} && U^2 \bullet \frac{V}{V_0} && \text{(a)}\\
&\text{subject to} && \left(\mathbf{K}_\mathrm{p}+\mathrm{i}\omega\mathbf{C}_\mathrm{p}-\omega^2\mathbf{M}_\mathrm{p}+\mathbf{K}_\mathrm{b}^{\mathrm{eq}}\right)\mathbf{u}_\mathrm{p}=\mathbf{f}_0, && \text{(b)}\\
& && g\left(\mathbf{u}_\mathrm{m}\left(\omega=0\right)\right)\le\overline{g}, && \text{(c)}\\
& && \underline{\rho}\le\rho_j\le 1,\ j=1,\ldots,N_\mathrm{d}. && \text{(d)}
\end{aligned} \tag{6}$$

5. SIMP model for topology optimization of plate structures

A single solid material is employed in the topology optimization of the base plate. As is well known, a transformed and relaxed continuous problem instead of the discrete 0/1 design problem is adopted by introducing some form of continuation and penalization. The classical SIMP (Solid Isotropic Material with Penalization) interpolation scheme [7, 8] is used in this study. The finite element stiffness and mass matrices of the *e*-th element in the design domain can be expressed as

$$\mathbf{k}_e\left(\rho_e\right)=\rho_e^p\mathbf{k}_e^0, \tag{7}$$

$$\mathbf{m}_e\left(\rho_e\right)=\rho_e^q\mathbf{m}_e^0, \tag{8}$$

respectively, where $\mathbf{k}_e^0$ and $\mathbf{m}_e^0$ denote the element stiffness and mass matrices corresponding to the given solid elastic material. Here, the symbols p and q are penalty parameters, and continuation of the penalization is adopted in the optimization iterations by gradually increasing p and q from 1.0 to 3.0. The same factors p =3 and q =3 for stiffness and mass matrices are finally used until convergence. In order to suppress the numerical instability and applying a minimum length constraint, the basic density filtering [9] is used in this paper.

6. Design sensitivity analysis

The sensitivities of the objective and constraint functions will be derived analytically in Sub-sections 6.1 and 6.2, respectively.

6.1. Sensitivity of objective function

From Eq.(1), the sensitivity of the objective function is computed as

$$\frac{\partial\left(U^2\bullet\dfrac{V}{V_0}\right)}{\partial\rho_k}=\frac{\partial\left(U^2\right)}{\partial\rho_k}\frac{V}{V_0}+\frac{U^2}{V_0}\frac{\partial\left(V\right)}{\partial\rho_k}, \tag{9}$$

where the sensitivity of the used material volume is computed as

$$\frac{\partial\left(V\right)}{\partial\rho_k}=v_j, \tag{10}$$

and the sensitivity of the squared displacement response U^2 is computed via the adjoint method. The following function is constructed after introducing Lagrangean multipliers $\boldsymbol{\lambda}$ and $\overline{\boldsymbol{\lambda}}$

$$L=U^2+\boldsymbol{\lambda}^\mathrm{T}\left[\mathbf{S}\mathbf{u}_\mathrm{p}-\mathbf{f}_0\right]+\overline{\boldsymbol{\lambda}}^\mathrm{T}\left[\overline{\mathbf{S}}\overline{\mathbf{u}}_\mathrm{p}-\overline{\mathbf{f}}_0\right], \tag{11}$$

where the dynamic stiffness matrix $\mathbf{S}$ is written as, cf. Eq. (6b),

$$\mathbf{S}=\mathbf{K}_\mathrm{p}+\mathrm{i}\omega\mathbf{C}_\mathrm{p}-\omega^2\mathbf{M}_\mathrm{p}+\mathbf{K}_\mathrm{b}^{\mathrm{eq}}. \tag{12}$$

Furthermore, we can obtain from the governing equation in Eq. (6b),

$$\mathbf{S}\mathbf{u}_\mathrm{p}=\mathbf{f}_0, \tag{13}$$

$$\bar{\mathbf{S}}\bar{\mathbf{u}}_{\mathrm{p}} = \bar{\mathbf{f}}_0 . \tag{14}$$

The design sensitivity can be analyzed as below if the loading $\mathbf{f}_0$ is assumed to be design independent

$$\frac{\partial L}{\partial \rho_k} = \frac{1}{N_{\mathrm{c}}} \frac{\partial \left(\mathbf{u}_{\mathrm{p}}^{\mathrm{T}} \mathbf{L} \bar{\mathbf{u}}_{\mathrm{p}} \right)}{\partial \rho_k} + \frac{\partial \boldsymbol{\lambda}^{\mathrm{T}}}{\partial \rho_k} \left[\mathbf{S}\mathbf{u}_{\mathrm{p}} - \mathbf{f}_0 \right] + \frac{\partial \bar{\boldsymbol{\lambda}}^{\mathrm{T}}}{\partial \rho_k} \left[\bar{\mathbf{S}}\bar{\mathbf{u}}_{\mathrm{p}} - \bar{\mathbf{f}}_0 \right] + \boldsymbol{\lambda}^{\mathrm{T}} \left[\frac{\partial \mathbf{S}}{\partial \rho_k} \mathbf{u}_{\mathrm{p}} + \mathbf{S} \frac{\partial \mathbf{u}_{\mathrm{p}}}{\partial \rho_k} \right] + \bar{\boldsymbol{\lambda}}^{\mathrm{T}} \left[\frac{\partial \bar{\mathbf{S}}}{\partial \rho_k} \bar{\mathbf{u}}_{\mathrm{p}} + \bar{\mathbf{S}} \frac{\partial \bar{\mathbf{u}}_{\mathrm{p}}}{\partial \rho_k} \right]. \tag{15}$$

After rearrangement and by setting the coefficient matrix of the terms with the derivative of displacement equal to zero, we obtain the sensitivity of the Lagrangean function

$$\frac{\partial L}{\partial \rho_k} = \boldsymbol{\lambda}^{\mathrm{T}} \left[\frac{\partial \mathbf{S}}{\partial \rho_k} \mathbf{u}_{\mathrm{p}} \right] + \bar{\boldsymbol{\lambda}}^{\mathrm{T}} \left[\frac{\partial \bar{\mathbf{S}}}{\partial \rho_k} \bar{\mathbf{u}}_{\mathrm{p}} \right], \tag{16}$$

which is equivalent to

$$\frac{\partial L}{\partial \rho_k} = 2\,\mathrm{Re}\left(\boldsymbol{\lambda}^{\mathrm{T}} \left[\frac{\partial \mathbf{S}}{\partial \rho_k} \mathbf{u}_{\mathrm{p}} \right] \right). \tag{17}$$

Eqs. (11) and (17) give

$$\frac{\partial U^2}{\partial \rho_k} = 2\,\mathrm{Re}\left(\boldsymbol{\lambda}^{\mathrm{T}} \left[\frac{\partial \mathbf{S}}{\partial \rho_k} \mathbf{u}_{\mathrm{p}} \right] \right). \tag{18}$$

The sensitivity of the objective function is easily derived using the result in Eqs. (18) and (9) and the harmonic motion assumption. The material interpolation formulas in Eqs. (7) and (8) are used for evaluating the derivatives of the stiffness and mass matrices.

6.2. Sensitivity of constraint functions

For the constraint on the static displacement of the machine, the constraint function $g\left(\mathbf{u}_{\mathrm{m}} \left(\omega = 0 \right) \right)$ is defined in Eq. (5), and expressed in terms of $\mathbf{u}_{\mathrm{m}}$, N_{m} and the location matrix $\mathbf{R}$, the sensitivity of the constraint function is computed as

$$\frac{\partial g}{\partial \rho_k} = \frac{1}{2} \frac{1}{\sqrt{\frac{1}{N_{\mathrm{m}}} \mathbf{u}_{\mathrm{p}}^{\mathrm{T}} \mathbf{R} \mathbf{u}_{\mathrm{p}}}} \frac{\partial \left(\frac{1}{N_{\mathrm{m}}} \mathbf{u}_{\mathrm{p}}^{\mathrm{T}} \mathbf{R} \mathbf{u}_{\mathrm{p}} \right)}{\partial \rho_k} = \frac{1}{2g} \frac{\partial \left(g^2 \right)}{\partial \rho_k} \tag{19}$$

The adjoint method is also used for deriving the design sensitivity of the function g^2, and the following function is constructed after introducing the Lagrangean multiplier for the excitation frequency $\omega = 0$,

$$L_g = g^2 + \boldsymbol{\alpha}^{\mathrm{T}} \left[\mathbf{K}\mathbf{u}_{\mathrm{p}} - \mathbf{f}_0 \right]. \tag{20}$$

where $\mathbf{K} = \mathbf{K}_{\mathrm{p}} + \mathbf{K}_{\mathrm{b}}^{\mathrm{eq}} \left(\omega = 0 \right)$, and the design sensitivity can be expressed as

$$\frac{\partial L_g}{\partial \rho_k} = \frac{1}{N_{\mathrm{m}}} \frac{\partial \left(\mathbf{u}_{\mathrm{p}}^{\mathrm{T}} \mathbf{R} \mathbf{u}_{\mathrm{p}} \right)}{\partial \rho_k} + \frac{\partial \boldsymbol{\alpha}^{\mathrm{T}}}{\partial \rho_k} \left[\mathbf{K}\mathbf{u}_{\mathrm{p}} - \mathbf{f}_0 \right] + \boldsymbol{\alpha}^{\mathrm{T}} \left[\frac{\partial \mathbf{K}}{\partial \rho_k} \mathbf{u}_{\mathrm{p}} + \mathbf{K} \frac{\partial \mathbf{u}_{\mathrm{p}}}{\partial \rho_k} \right]. \tag{21}$$

By setting the coefficient matrix of the terms with the derivative of displacement equal to zero, and making use of of the symmetry of the stiffness matrix $\mathbf{K}$ and the location matrix $\mathbf{R}$, we obtain

$$\frac{\partial L_g}{\partial \rho_k} = \boldsymbol{\alpha}^{\mathrm{T}} \frac{\partial \mathbf{K}}{\partial \rho_k} \mathbf{u}_{\mathrm{p}} . \tag{22}$$

The sensitivity of the constraint function *g* is now easily derived from Eqs. (22) and (19)

$$\frac{\partial g}{\partial \rho_k} = \frac{1}{2g} \boldsymbol{\alpha}^{\mathrm{T}} \frac{\partial \mathbf{K}}{\partial \rho_k} \mathbf{u}_{\mathrm{p}} . \tag{23}$$

With these sensitivity results, the optimization problem in Eq. (6) may be solved by a mathematical programming method, e.g., the Method of Moving Asymptotes (MMA) by Svanberg[10]. The convergence criterion is specified as follows. When the maximum relative change of the design variables in two consecutive iterations is smaller than a specified value, e.g. 0.01, or the relative change of the values of the objective function in two consecutive iterations is smaller than a specified value, e.g. 1e-5, the optimization iterations are stopped.

7. Numerical examples: minimization of the product of the building vibration transmission and the volume of base plate material

Building 3-3 as shown in Figure 1 is considered with the dimensions of a room chosen as: length L = 6 m, height H = 3.6 m, and width W = 4.8 m. The base plate with the machine is installed on top of Room 2-3 through the hinges in the corners of the quadratic design domain for the base plate with continuity of only the translational degrees of freedom, and the equivalent complex stiffness matrix of the building is computed correspondingly at the four installation points for each given excitation frequency. The machine is assumed to be installed at the centre of the base plate by four rigid mounts, where the translational and rotational degrees of freedom are fully coupled. In the following examples, an excitation loading is applied at the centre of gravity of the machine with the amplitude vector $\mathbf{f}_0 = \{0, 0, 1000\}^{\mathrm{T}}$, i.e., 1000 N in the vertical *z*-direction. The geometric and material parameters of the base plate and the machine are listed in Table 1 and Table 2, respectively. The base plate is meshed into 96×96 nine-node Mindlin plate elements with three degrees of freedom per node, where the in-plane motion is ignored.

Table 1 Geometric and material properties of the base plate

Base plate (Aluminum)	
Dimension of the plate:	1.2 m × 1.2 m
Young's modulus	73.1×10^9 Pa
Mass density	2700 kg/m^3
Thickness	0.02 m
Meshing	96×96 nine-node elements

Table 2 Material and geometric parameters of the machine

Machine (3D elastic body, made by steel)	
Length	0.2 m
Width	0.2 m
Height	0.1 m
Young's modulus	210×10^9 Pa
Mass density	7800 kg/m^3
Mass	0.2×0.2×0.1×7800 = 31.2 kg

7.1. Numerical examples

In this subsection, the topology optimization of the base plate is studied by assuming no damping for the base plate and the building structures. Free vibration analysis is first performed for the system including the building, the machine, and the initial base plate. Here, the initial design of the base plate is defined by all the (density) design variables of the admissible design domain being equal to 0.5, which is regarded as a reference design for comparison. The eigenfrequencies and eigenmodes of the building system with the initial base plate are presented in Figure 3, where the first eigenfrequency is 9.312 Hz.

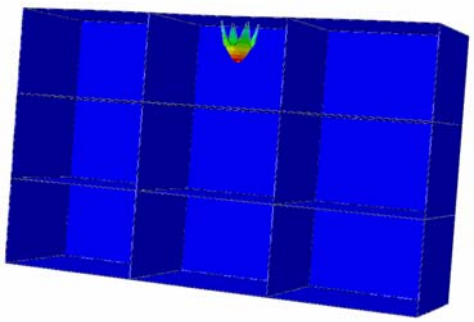

(a) Mode 1, f_1^{eg} = 9.312 Hz

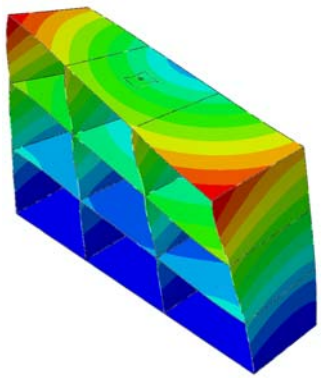

(b) Mode 2, f_2^{eg} =12.469 Hz

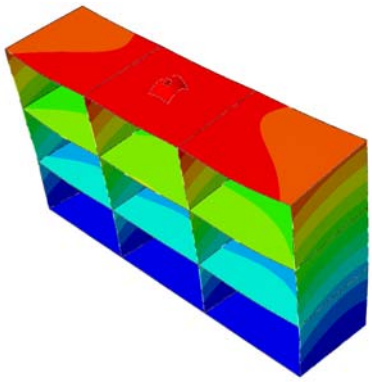

(c) Mode 3, f_3^{eg} = 13.200 Hz

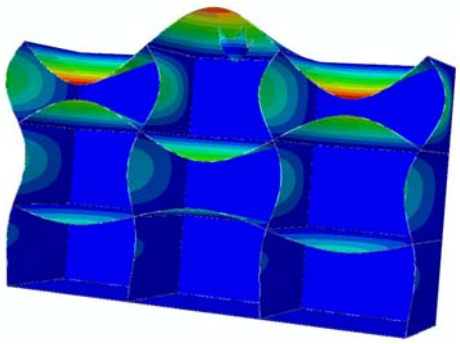

(d) Mode 4, f_4^{eg} =19.089 Hz

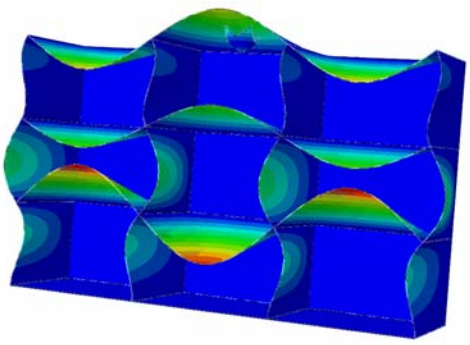

(e) Mode 5, f_5^{eg} =20.153 Hz

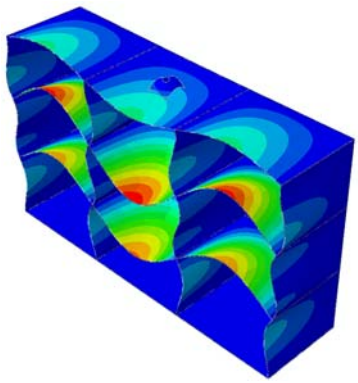

(f) Mode 6, f_6^{eg} =21.240 Hz

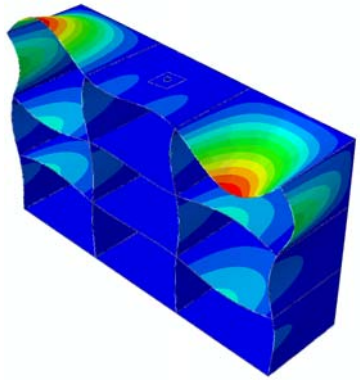

(g) Mode 7, f_7^{eg} =21.969 Hz

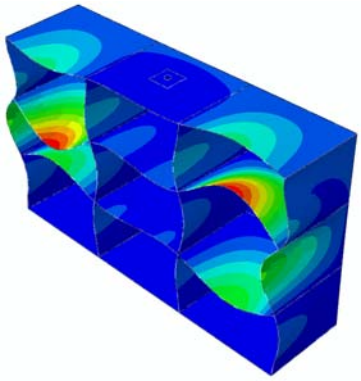

(h) Mode 8, f_8^{eg} =22.885 Hz

Figure 3 Eigenfrequencies and eigenmodes of the building system with the initial base plate (a-h). Red colour represents larger (numerical) displacement magnitude, and blue represents zero displacement.

Then, design optimization for minimizing the product of the vibration transmission and the used volume of material formulated in Eq. (6) is carried out for different single excitation frequencies, f = 5, 20, 40 Hz. Different upper limits $\bar{g}$ of the RMS value of the maximum allowable static displacements is studied, e.g., $\bar{g}$ =3 mm, and $\bar{g}$ =5 mm. The density filter radius is two times the length of the plate element.

(a) Excitation frequency f = 5 Hz (b) Excitation frequency f = 20 Hz (c) Excitation frequency f = 40 Hz

Figure 4 Optimized topologies of the base plate with excitation at different frequencies for minimizing the product of the vibration transmission in Building 3-3 and the volume of material used for the base plate. Given upper limit on the static displacement of the machine: $\bar{g}$ =3 mm: (a) excitation frequency f = 5 Hz, (b) f = 20 Hz, (c) f = 40 Hz

Table 3 Comparison of the objective, the squared displacement response at the installation positions, and the amount of used material for the reference and the optimized designs in Figure 4(a-c)

	$U^2 \bullet \frac{V}{V_0}$		Relative decrease of objective	U^2		$\frac{V}{V_0}$	
	Reference	Optimized		Reference	Optimized	Reference	Optimized
Figure 4(a) at f = 1 Hz	7.3684e-9	4.2297e-10	94.26%	1.4737e-8	1.2702e-9		0.333
Figure 4(b) at f = 20 Hz	1.1154e-10	2.7149e-11	75.66%	2.2308e-10	8.6462e-11	0.5000	0.314
Figure 4(c) at f = 40 Hz	7.4397e-11	2.7326e-12	96.33%	1.4879e-10	7.7411e-12		0.353

(a) Excitation frequency f = 5 Hz (b) Excitation frequency f = 20 Hz (c) Excitation frequency f = 40 Hz

Figure 5 Optimized topologies of the base plate with excitation at different frequencies for minimizing the product of the vibration transmission in Building 3-3 and the volume of material used for the base plate. Given upper limit on the static displacement of the machine: $\bar{g}$ =5 mm: (a) excitation frequency f = 5 Hz, (b) f = 20 Hz, (c) f = 40 Hz

Table 4 Comparison of the objective, the squared displacement response at the installation positions, and the amount of used material for the reference design and the optimized designs in Figure 5(a-c)

	$U^2 \bullet \frac{V}{V_0}$		Relative decrease of objective	U^2		$\frac{V}{V_0}$	
	Reference	Optimized		Reference	Optimized	Reference	Optimized
Figure 5(a) at f = 5 Hz	7.3684e-9	9.6781e-11	98.69%	1.4737e-008	4.0494e-010		0.239
Figure 5(b) at f = 20 Hz	1.1154e-10	7.5232e-12	93.26%	2.2308e-010	3.6344e-011	0.5	0.207
Figure 5(c) at f = 40 Hz	7.4397e-11	6.1526e-13	99.17%	1.4879e-010	2.3217e-012		0.265

The optimized topologies of the base plate at the excitation frequencies f = 5, 20, and 40 Hz are shown in Figure 4(a-c) for $\bar{g}$ =3 mm and Figure 5(a-c) for $\bar{g}$ =5 mm. For the optimized designs, the constraint on the static displacement of the machine is always active. As a comparison, the squared displacement response U^2 for the reference base plate is computed for different cases. The values of the objective function, the volume ratio and the squared displacement response at different excitation frequencies for the reference and the optimized base plates in Figure 4(a-c) and Figure 5(a-c) are listed in Table 3 and Table 4, respectively, where it is seen that the objective has generally been decreased quite substantially for the optimized designs relative to the reference design in all the examples. The optimization has decreased the vibration transmission into buildings, and simultaneously reduced the amount of used material for the excitation frequencies f = 5, 20, and 40 Hz.

8. Conclusions

Vibration transmission in lightweight buildings is minimized by design optimization of the base plate of machinery at different frequencies. Minimization of the product of the vibration transmission into the building and the volume of material used in the base plate is chosen as the design objective. Since the minimization of the vibration transmission would like to separate the building from the machinery, which results into a trivial solution, a constraint on the static displacement of the machinery is introduced in order to provide a practically meaningful design.

Optimized topologies of the base plate are obtained for different excitation frequencies and different static displacement constraints. For low frequencies, the designs are stiffness-driven. Since the building floors can be considered relatively stiff in the low frequency range, the optimum topologies are very similar for different installation positions in the building. For larger excitation frequencies, the vibration of the building floor has more influence on the vibration mode of the base plate and the vibration transmission into the building. For excitation frequencies larger than the first eigenfrequency of the base plate, the topologies become more mass-driven and generally exhibit some concentration of mass in the central area. The influence on the optimum base plate topology of material damping and of different base plate installation positions in the building, is subject to further study.

9. Acknowledgements

This work has been funded by the EU InterReg Project “Silent Spaces” and Aalborg University.

10. References

[1] B. Niu, N. Olhoff, G. Cheng, Topological design for minimization of the product of dynamic compliance and material cost for structures subjected to forced vibration in a range of excitation frequencies, 2013, in preparation.

[2] G.I.N. Rozvany, O.M. Querin, Z. Gaspar, V. Pomezanski, Extended optimality in topology design, *Structural and Multidisciplinary Optimization*. 24, 257-261, 2002.

[3] G.I.N. Rozvany, A critical review of established methods of structural topology optimization, *Structural and Multidisciplinary Optimization*. 37, 217-237, 2009.

[4] G.I.N. Rozvany, Traditional vs. Extended optimality in topology optimization, *Structural and Multidisciplinary Optimization*. 37, 319-323, 2009.

[5] L.V. Andersen, P.H. Kirkegaard, K. Persson, N. Kiel, B. Niu, A modular finite-element model for analysis of vibration transmission in multi-storey lightweight buildings, *Proceedings of the Eleventh International Conference on Computational Structures Technology (CST2012)*, Civil-Comp Press, Dubrovnik, Croatia, 2012.

[6] B. Niu, L.V. Andersen, N. Kiel, O. Flodén, G. Sandberg, Vibration transmission in a multi-storey lightweight

building: A parameter study, *Proceedings of the Eleventh International Conference on Computational Structures Technology (CST2012)*, Civil-Comp Press, Dubrovnik, Croatia, 2012.
[7] M.P. Bendsøe, Optimal shape design as a material distribution problem, *Structural Optimizatio*n. 1, 193–202, 1989.
[8] G. Rozvany, M. Zhou, T. Birker, Generalized shape optimization without homogenization, *Structural Optimization*. 4, 250-252, 1992.
[9] T.E. Bruns, D.A. Tortorelli, Topology optimization of non-linear elastic structures and compliant mechanisms, *Computer Methods in Applied Mechanics and Engineering*. 190, 3443-3459, 2001.
[10] K. Svanberg, The method of moving asymptotes - a new method for structural optimization, *International Journal for Numerical Methods in Engineering*. 24, 359-373, 1987.